Bioactivity of wollastonite/aerogels composites obtained from a TEOS–MTES matrix

Jose Antonio Toledo-Fernández · Roberto Mendoza-Serna · Victor Morales · Nicolás de la Rosa-Fox · Manuel Piñero · Alberto Santos · Luis Esquivias

Abstract Organic–inorganic hybrid materials were synthesized by controlled hydrolysis of tetraethoxysilane (TEOS), methyltrimethoxysilane (MTES), synthetic wollastonite powders and polydimethylsiloxane (PDMS) in an ethanol solution. Aerogels were prepared from acid hydrolysis of TEOS and MTES with different volume ratio in ethanol, followed by addition of wollastonite powder and PDMS in order to obtain aerogels with 20 wt% of PDMS and 5 wt% of CaO of the total silica. Finally, when the wet gels were obtained, they were supercritically dried at 260 °C and 90 bar, in ethanol. In order to obtain its bioactivity, one method for surface activation is based on a wet chemical alkaline treatment. The particular interest of this study is that we introduce hybrid aerogels, in a 1 M solution of NaOH, for 30 s at room temperature. We evaluate the bioactivity of TEOS–MTES aerogel when immersed in a static volume of simulated body fluid (SBF). An apatite layer of spherical-shaped particles of uniform size smaller than 5 microns is observed to form on the surface of the aerogels after 25 days soaking in SBF.

J. A. Toledo-Fernández · R. Mendoza-Serna (✉) ·
V. Morales · N. de la Rosa-Fox
Departamento Física de la Materia Condensada, Facultad de Ciencias, Universidad de Cádiz, Avenida República Saharaui, s/n, 11510 Puerto Real, Cadiz, Spain
e-mail: roberto.serna@uca.es
URL: http://www.uca.es/grup-invest/geles/

M. Piñero
Departamento de Física Aplicada, CASEM, Universidad de Cádiz, Puerto Real, Cadiz, Spain

A. Santos
Departamento de Cristalografía y Mineralogía, CASEM, Universidad de Cádiz, 11510 Puerto Real, Cadiz, Spain

L. Esquivias
Departamento de Física de la Materia Condensada, Facultad de Física, Instituto de Ciencia de Materiales de Sevilla (CSIC), Universidad de Sevilla, Seville, Spain

1 Introduction

Organic–inorganic hybrid materials (OIHM) obtained from tetraethoxysilane and methyltriethoxysilane (TEOS–MTES systems) have been extensively studied as matrices for different functional molecules. They offer many potential applications as porous films with low dielectric constant, hydrophobic membranes with very high gas permeability for CO_2, and coatings with interesting mechanical properties [1–5]. OIHM obtained from TEOS, MTES and poly-dimethyl-siloxane (PDMS) present a lower porosity and higher rupture strength than TEOS–MTES gels, and can be used for their optical, electrical and catalytic properties [6].

Porous bioactive glasses are potentially useful materials for orthopaedic applications. Their porosity is an important characteristic since it allows vascular penetration and subsequent neo-bone growth. A high surface-to-volume ratio helps to make these materials biodegradable and bioactive, permitting an apatite-like layer to grow when in contact with body fluid [7].

Silica gels derived from the sol–gel process have a high surface area and porosity and have been shown to be far more effective in inducing hydroxyapatite formation than either silica glass or quartz [8]. The textural properties play a crucial role in governing the bioactivity of these materials. Silica aerogels are nanostructured, transparent, chemically inert and highly porous materials. The density of these aerogels may vary from 0.0019 g cm^{-3} to 0.9 g cm^{-3} [9], with a high porosity, close to 90%, with pores of

nanometric size that give rise to specific surfaces of between 600 and 1,000 $m^2 g^{-1}$, and their composition stays identical to that of vitreous silica [10, 11]. Their main limitations are fragility and high hygroscopicity.

In recent years, organically-modified ceramics from gels have been attracting much attention as a new family of hybrid materials. In these materials, organic polymers are chemically incorporated into the inorganic network at the molecular level. As a result, unique mechanical properties can be derived, particularly a low elastic modulus and high ductility combined with high mechanical strength. It is widely believed that such hybrid materials present unique applications as a new kind of bioactive material [12].

Wollastonite is a natural calcium silicate, which has been used extensively as filler in polymers and cements, to fabricate composites with improved mechanical properties. Recent studies have shown that wollastonite is bioactive and degradable; consequently it has potential use as a bioactive material in tissue repair or tissue engineering research [13].

Different metal pre-treatment and coating methods, such as alkaline or acid treatment, or using H_2O_2, and sol–gel coating of TiO_2, have been used by various research groups in an attempt to form such a bioactive surface on Ti plates. Kim et al. [14] reported that amorphous sodium titanate hydrogel, obtained by exposing pure Ti to an alkaline solution and subsequently to heat treatment, would induce apatite formation when soaked for a period of time in SBF. They showed that pure Ti metal formed a bonelike apatite layer on its surface in SBF within 3 days after being prepared, by soaking in a 5 M solution of NaOH at 60 °C for 24 h with subsequent heat treatment at 600 °C for 1 h [15]. Other authors have reported that, in order to induce nucleation of the Ti with 1–20 M solutions of NaOH, it was exposed to temperatures of 60–95 °C for 24 h. In some cases it has been concluded that the immersion in a 5 M solution of NaOH at 80 °C for 24 h is the optimum treatment [16, 17].

The objective of the present study is to synthesize hybrid bioactive aerogels, whose inorganic phase is SiO_2 and the organic phase is PDMS and the methyl groups that remain bound to silicon after the MTES hydrolysis. Synthetic wollastonite powders are used as the bioactive phase. They received a surface treatment that induces the formation of the hydroxyapatite nucleus. This treatment consisted of maintaining the aerogels in an alkaline solution (NaOH, 1 M) at room temperature for 30 s. Studies of the resulting bioactivity and mechanical properties were also carried out, and the results were compared with those for human cancellous bone to evaluate its potential application for bone substitution or regeneration.

2 Materials and methods

2.1 Sample preparation

Silica-based organic–inorganic hybrid gels were synthesized by the classic sol–gel method using a two-step procedure. First, TEOS and MTES (both reagents from Merck, Germany; purity ≥99%), were used as inorganic and organic phase precursors, respectively. We have combined different amounts of TEOS and MTES, with the following TEOS:MTES volume ratios: 9:1, 5:5 and 1:9. They were hydrolysed under-stoichiometrically with acidic water (pH ∼1) in a molar ratio [TEOS + MTES]: [H_2O] = 1:0.84. At this stage, 320 J cm^{-3} of ultrasound was applied to the mix from a device delivering 0.6 w cm^{-3} of ultrasound power energy to the system, giving a transparent and homogeneous solution.

In the second step, silanol-terminated poly-dimethyl-siloxane (PDMS) with quoted average molecular weight of 400–700 g mol^{-1} (ABCR, USA; 99.5%) was used as the polymer component. This organic polymer was added (drop by drop, under the action of 320 J cm^{-3} of ultrasound) in a molar ratio [TEOS]:[DMS] = 1:0.027 (representing ∼20% by weight of PDMS with respect to the final amount of silica), where the organic fraction has been expressed as a function of the dimethyl-siloxane monomer, DMS. Then the sol was left in an oven for 24 h at 50 °C. The mix was hydrolysed (pH ∼1) with HNO_3 catalyst (Panreac, Spain; purity 60% by vol.) in a molar ratio [TEOS]:[H_2O] = 1:3.16, again applying 320 J cm^{-3} of ultrasound energy. Synthetic wollastonite powders ($CaSiO_3$) [9] were used as a bioactive phase. The appropriate amount of wollastonite (to give a Ca content of 5% by weight with respect to the total amount of silica) was dispersed in 75 ml of EtOH per gram of wollastonite and then added to the precursor sol under sonication (320 J cm^{-3}). The mixture was poured into a polyethylene container before gelation, which occurs in approximately one minute, thus preventing the powder from settling. Then the container was left in an oven at 50 °C for 24 h. Next, the alkogels were soaked in ethanol at room temperature for 7 days for aging and removing the residual water from the pores.

At this point the gel is placed in an autoclave and the pore liquor is vented-off above the supercritical conditions of ethanol (240 °C, 63 bar). The supercritical state is attained by slow heating (1 °C/min) in order to minimize the ethanol thermal expansion coefficient, which is much greater than that of the wet silica gel network. Then the heating produces the evaporation of the additional volume of ethanol that allows the supercritical pressure and temperature (255 °C, 85 bar) to be reached, in such a way that the vapour–liquid equilibrium curve is never crossed, to

avoid capillary pressures on the adjacent pore. Thus the structure does not collapse and the aerogel retains its original shape. As a provision for the mechanical test, samples were made as cylinders of approximately 18 mm length and 8 mm diameter. Density was calculated by weighing the sample with a well-defined geometry.

In order to facilitate the bioactivity of aerogels, we applied an alkaline treatment to the surface of the samples, without damaging the material. In our case, we treated the aerogels with NaOH (1 M) for 30 s at room temperature. A porous surface layer adheres strongly to the aerogel, as the result of the increased number of OH terminating groups on the surface. It is well-known that the presence of OH groups seems to facilitate the bonding of the aerogel to the apatite layer. It was expected that the use of the alkaline treatment would makes the aerogel surface hydrophilic. This condition plays a very important role in the formation of the apatite. After this treatment, the samples were gently washed in distilled water and dried in a desiccator for 24 h.

The composites were designated in the style S20Ca5x. The values 20 and 5 refer, respectively, to the PDMS and Ca content of the composite matrix; x indicates that the TEOS:MTES volume ratio is x:(10 − x).

2.2 Bioactivity test

In order to evaluate the bioactivity, the aerogels previously treated with NaOH were immersed in sterile polyethylene boxes containing 35 ml of SBF (Table 1) at 37 °C for 25 days according to the procedure proposed by Kokubo et al. [18]. The SBF was prepared by dissolving reagent grade NaCl, NaHCO$_3$, KCl, K$_2$HPO$_4$ · 3H$_2$O, MgCl$_2$ · 6 H$_2$O, CaCl$_2$, Na$_2$SO$_4$ in distilled water, and buffering the solution to pH 7.4 with tris-hydroxymethyl-aminomethane ((CH$_2$OH)$_3$CNH$_3$) and 1.0 M HCl at 37 °C. Then the aerogels were rinsed with distilled water and dried in a desiccator for 24 h.

Table 1 Ion concentrations of human blood plasma and SBF

Ion	Concentration/mM	
	Blood plasma	SBF
Na$^+$	142.0	142.0
K$^+$	5.0	5.0
Mg^{2+}	1.5	1.5
Ca^{2+}	2.5	2.5
Cl$^-$	103.0	147.8
HCO$_3^-$	27.0	4.2
HPO$_4^{2-}$	1.0	1.0
SO$_4^{2-}$	0.5	0.5
pH	7.2–7.4	7.40

The Kokubo's solution contains the inorganic components of the human blood plasma in similar concentrations. Several authors report that in vitro experiments with Kokubo's solution can satisfactorily reproduce in vivo behaviour of implant materials [19].

2.3 Examination of bioactivity and mechanical response

Three composites were synthesized: S20Ca5M1, S20Ca5M5 and S20Ca5M9. They were characterized structurally and texturally, and their bioactive and mechanical behaviours were evaluated to study the influence of the MTES content on the performance of the composite.

The thermogravimetric (TG) study was carried out in a Setaram Setsys 1750 by heating the samples in air from 25 °C to 1,000 °C at 10 °C/min. The average pore diameter and surface area of the composites were determined by N$_2$ adsorption/desorption isotherms at 77 K carried out in a Sorptomatic 1990 unit (CE Instruments).

To evaluate the bioactivity, the formation of apatite-like layers on the sample surfaces was monitored by scanning electron microscopy (SEM) in a FEI Sirion electron microscope coupled to an EDAX Genesis system. The Fourier Transform Infrared (FTIR) spectra of the aerogels were recorded before and after soaking, using a Bruker Vertex70 spectrophotometer with a resolution of 4 cm^{-1} in the 2,000–400 cm^{-1} region. Pellets were prepared by grinding the samples in an agate mortar and then mixing the powder with anhydrous KBr in a weight ratio of KBr:sample = 100:1.

The X-ray diffraction pattern (XRD) measurements were performed using a Bruker AXS D8 Advance diffractometer by the step-scanning method with Cu K$_\alpha$ radiation, a scan range from 20 to 50° 2θ, with a step of 0.2°, and a counting time of 1 s per step; the instrument was operated at 40 kV and 40 mA.

The strains at failure of the aerogels were evaluated at room temperature under compression using an AG-I machine (Shimadzu); the Young's moduli were calculated from the slope of the initial linear elastic portion of the stress–strain curve. The S20Ca5M1 sample has been submitted to a creep test [20, 21] applying 1.00 MPa for 4 h at room temperature. Creep compliance data were calculated directly, following the standard procedure [22, 23], as the strain divided by the applied stress.

3 Results and discussion

The thermograms of the S20Ca5M1, S20Ca5M5 and S20Ca5M9 samples are represented in Fig. 1. The three
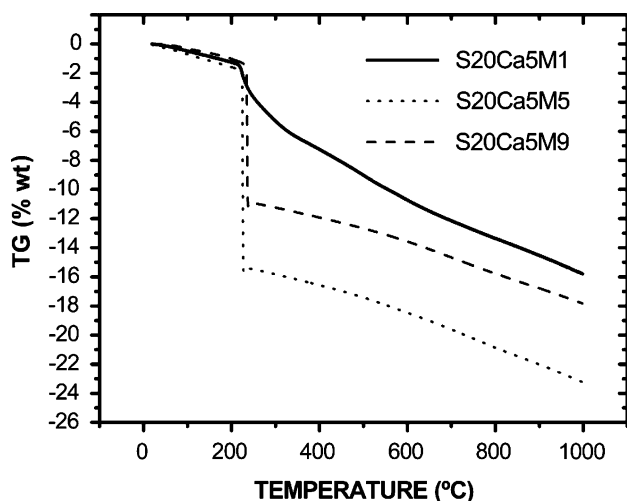
Fig. 1 TG curves of aerogels before soaking in SBF

Table 2 Textural data for the composites

Aerogel	BET surface area (m^2/g)	Pore volume (cm^3/g)	Average pore diameter (nm)
S20Ca5M1	856	3.11	9.8
S20Ca5M5	582	1.02	7.5
S20Ca5M9	271	0.69	10

composites present a sharp weight loss due to the carbonation of the organic polymer enduring after supercritical ethanol drying. The weight loss is greater in the S20Ca5M5 sample because the polymer is better encapsulated in the silica network formed by the TEOS and the MTES. This weight loss is 23% whereas for the S20CaM1 sample the loss is 16%.

These materials exhibited characteristics of type IV and V isotherms (Fig. 2) that correspond to mesoporous
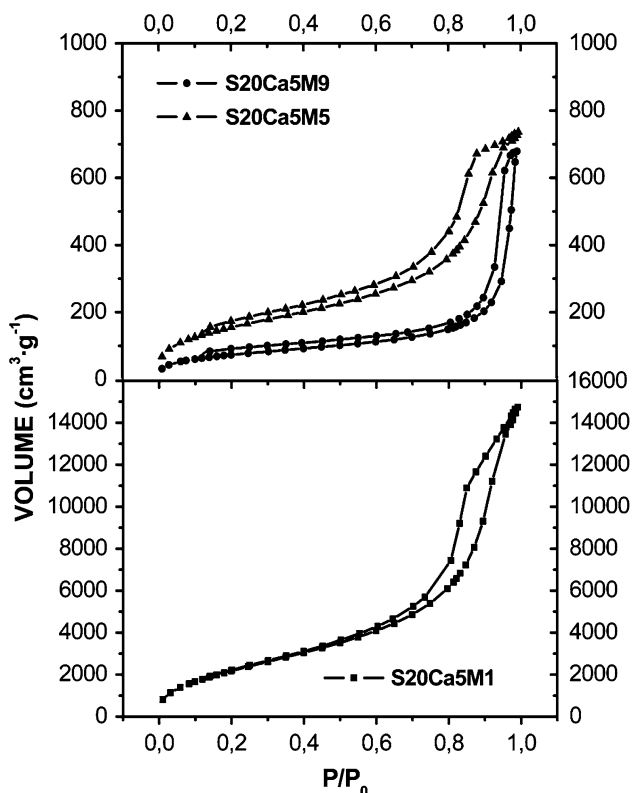
Fig. 2 Nitrogen adsorption/desorption isotherms of aerogels

materials, in which the N$_2$ adsorption at low pressure is produced by the formation of multiple layers. At high pressure, the adsorption is caused by capillary condensation, which is characterised by a clear hysteresis loop occurring in the mesoporous range. A transition is observed in the hysteresis loops from H4 to H3 type (which admittedly are quite similar) which indicates the presence of pores formed by flattened particles and slit-shaped pores [24]. The type H4 loop was reported for MCM−41 that exhibited particles with internal voids of irregular shape and broad size distribution (between 5 and 30 nm) [25]. This loop seems to be due merely to the existence of mesopores formed by the organic phase embedded within the inorganic phase containing relatively few micropores. Microporosity is a characteristic of the silica aerogels prepared with ultrasounds (known as sonogels) [26], which is modified by the presence of the organic phase [27, 28]. The textural properties extracted from the data analysis are given in Table 2.

Figure 3 presents SEM images and EDS spectra of the surface of hybrid S20Ca5M1 after immersion in SBF for 25 days. A layer covers the surface (Fig. 3a). As the magnification increases, rough spherical shaped particles can be observed (Fig. 3b, c), formed by fine lamellar crystals (Fig. 3d).

A semi-quantitative yield analysis indicates a Ca to P ratio of 1.70, almost the same composition as apatite [29, 30]. The S20Ca5M5 and S20Ca5M9 samples did not show significant bioactivity.

The FTIR spectra of the S20Ca5M1 sample before and after soaking in SBF are shown in Fig. 4a, b, respectively. The bands at 450 cm^{-1} are characteristic of O–Si–O bending vibration [31]. The bands at 1,268 and 803 cm^{-1} are assigned to Si–CH$_3$ bond of PDMS [32] and MTES [6, 33], the band at 850 cm^{-1} is due to TEOS−PDMS copolymerization [34]. In Fig. 4b, after soaking the composite for up to 25 days in SBF, the bioactive aerogel showed a typical doublet at 564 and 603 cm^{-1}, which can be ascribed to P–O bending vibration [35, 36]. A specific peak of HPO$_4^{2-}$ [37] appears at 875 cm^{-1}.

Figure 5 displays the diffracted X-ray intensities of the S20Ca5M1 composite after soaking in SBF for 25 days. The characteristic diffraction peaks of hydroxyapatite (HAp) were identified, confirming the bioactivity of this

Fig. 3 SEM micrograph and EDS pattern of S20Ca5M1 aerogel after soaking in SBF for 25 days
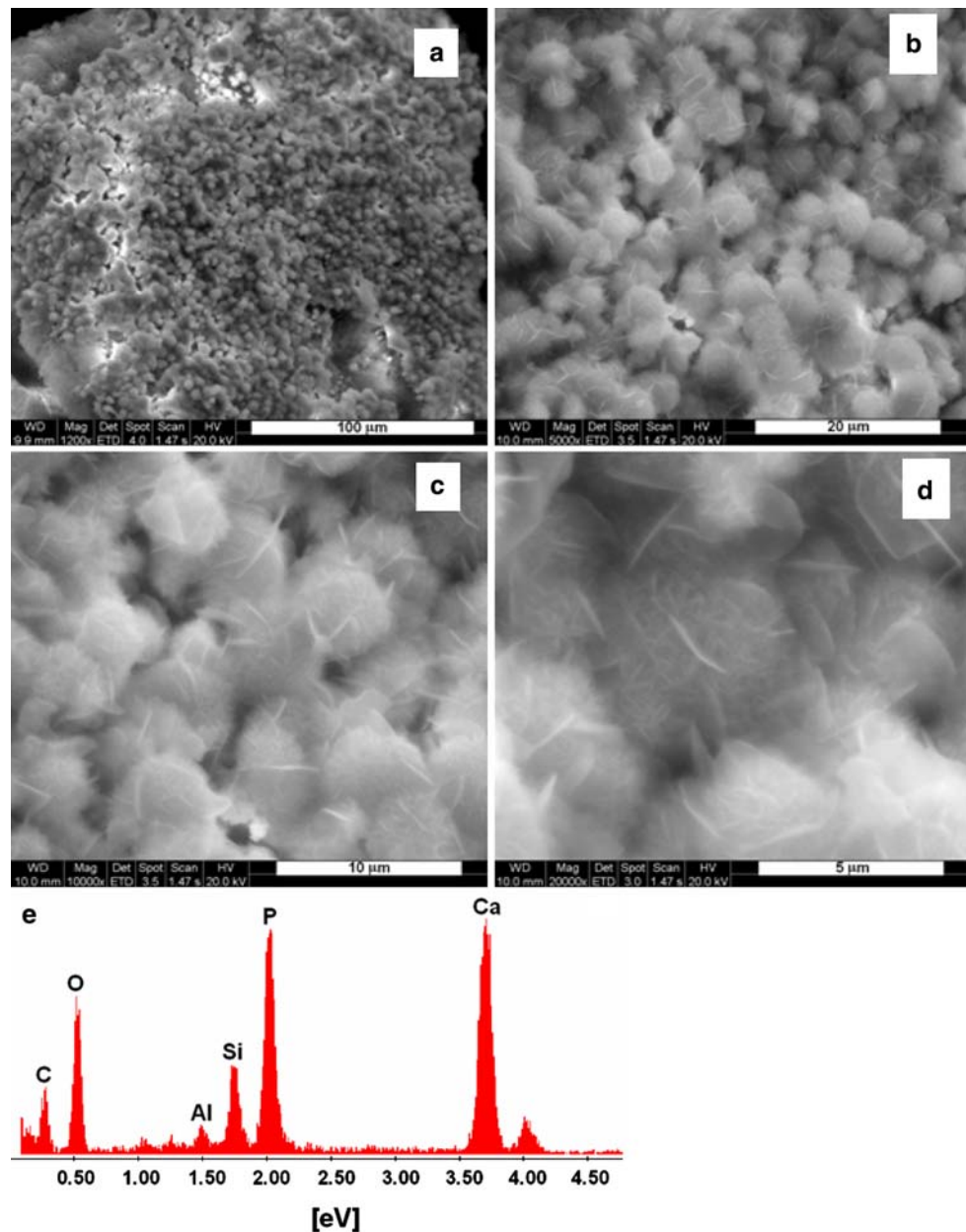
material [38–41] in agreement with the SEM, EDAX and FTIR observations.

Table 3 gives the values of both the Young's modulus and rupture strengths from the uniaxial compression test. The rupture modulus and Young's modulus increase as the content of MTES increases. For a better characterization of the visco–elastic behaviour of the material, we have calculated the Young modulus in three different intervals of the stress–strain curves: (a) in the elastic range (strain between 0 and 0.10), (b) in the middle of the visco–elastic behaviour (0.10–0.30) and, finally, (c) near the rupture limit (0.30–rupture strain). It can be seen that samples show an elastomer-like behaviour, as the Young's modulus increases as the strain approaches the rupture limit,

attaining a value as high as 117 MPa for the S20Ca5M9 sample. The three types of samples studied in this work present values of the Young's and rupture modulus in the standard range for human cancellous bone, i.e. 50–500 MPa [42, 43].

A bi-exponential fitting of the creep compliance of the S20Ca5M1 sample was carried out and is represented in Fig. 6. The satisfactory agreement between experimental data and theoretical expression indicates the existence of two different mechanisms of the time response. The exponents characterize the short-term and long-term responses. Their values are approximately 1,500 s and 20,000 s, respectively, and the creep compliance value is close to 0.11 GPa^{-1}, quite similar to that of the pure silica
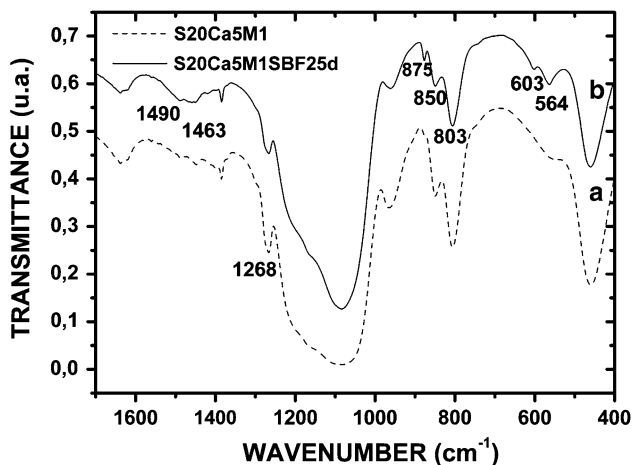
Fig. 4 FTIR spectra of S20Ca5M1 aerogel after and before soaking in SBF
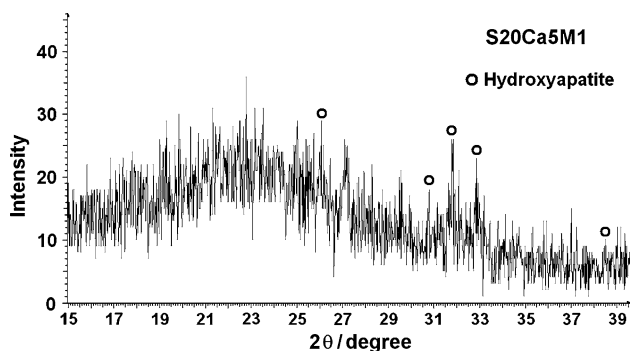

Fig. 6 Experimental creep compliance and biexponential fitting of sample S20Ca5M1 from creep test of 10 h

Fig. 5 X-ray powder diffraction patterns of aerogel

Table 3 Mechanical data for the composites

Sample	Rupture modulus (MPa)	Young's modulus (MPa)		
		A	B	C
S20Ca5M1	4	11	6	10
S20Ca5M5	5	29	38	61
S20Ca5M9	28	84	58	117

Strain intervals (%)

A: 0–10, B: 10–30, C: 30-Rupture

aerogel measured by nanoindentation (0.1 GPa^{-1}) [44]. This can be explained on the basis of a response mechanism controlled by the inorganic phase skeleton.

4 Conclusions

The specific features of these hybrid aerogels: weight loss, specific surface and mechanical properties can be directly attrib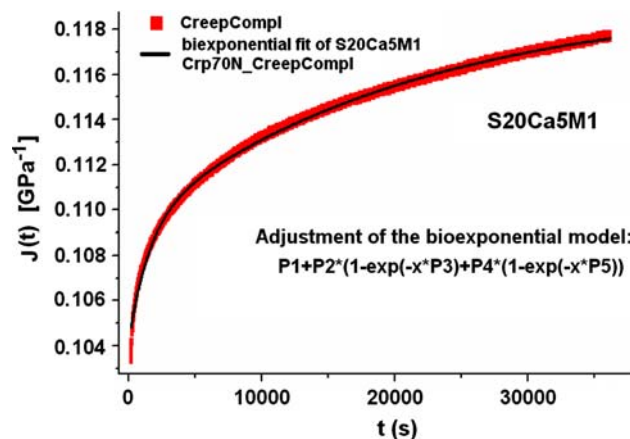uted to the MTES content. The treatment to induce bioactivity proved to be appropriate for obtaining bioactive materials. The aerogel S20Ca5M1 is expected to find application as a new type of bioactive material, having demonstrated an excellent apatite-forming ability in SBF, and mechanical properties analogous to those of human cancellous bone.

References

1. S. YU, T. K. S. WONG, X. HU and T. K. GOH, *Thin Solid Films* **462–463** (2004) 306
2. R. GHISLENI, D. A. LUCCA, M. NASTASI, L. SHAO, Y. Q. WANG, J. DONG and A. MEHNER, *Nucl. Instr. Meth. B* (2007), doi:10.1016/j.nimb.2007.01.061
3. R. M. DE VOS, W. F. MAIER and H. VERWEIJ, *J. Non-Cryst Solids* **158** (1999) 277
4. N. K. RAMAN and C. J. BRINKER, *J. Membrane Sci.* **105** (1995) 273
5. S. PELLICE, U. GILABERT, C. SOLIER, Y. CASTRO and A. DURAN, *J. Non-Cryst. Solids* **348** (2004) 172
6. Z. CHANG, L. AÍMEI, Z. XIAO, F. MIAO, H. JUAN and Z. HONGBING, *Opt. Mater.* (2006), doi:10.1016/j.optmat.2006.08.014
7. Â. L. ANDRADE, P. VALERIO, A. M. GOES, M. F. LEITE and R. Z. DOMINGUES, *J. Non-Cryst. Solids* **352** (2006) 3508
8. R. VITALA, J. SIMOLA, T. PELTOLA, H. RAHIALA, M. LINDEN, M. LANGLET and J. B. ROSENHOLM, *J. Biomed. Mater. Res.* **54** (2001) 109
9. J. A. TOLEDO-FERNÁNDEZ, R. MENDOZA-SERNA, V. MORALES-FLÓREZ, N. DE LA ROSA-FOX, A. SANTOS, M. PIÑERO and L. ESQUIVIAS, *Bol. Soc. Esp. Ceram. V* **46**(3) (2007) 138

10. J. FRICKE and T. TILLOTSON, *Thin Solid Films* **297** (1997) 212

11. N. HÜSING and U. SCHUBERT, In *Aerogels-Airy Materials: Chemistry, Structure and Properties* (Angew. Chem. Int., German, 1998) p. 22

12. Q. CHEN, F. MIYAJI, T. KOKUBO and T. NAKAMURA, *Biomaterials* **20** (1999) 1127

13. H. LI and J. CHANG, *Biomaterials* **25** (2004) 5473

14. H. M. KIM, F. MIYAJI, T. KOKUBO and T. NAKAMURA, *J. Ceram. Soc. Jpn.* **105** (1997) 121

15. M. WEI, H.-M. KIM, T. KOKUBO and J. H. EVANS, *Mat. Sci. Eng. C* **20** (2002) 125

16. J.-H LIN, C.-H. CHANG, Y.-S. CHEN and G. T. LIN, *Surf. Coat. Technol.* **200** (2006) 3665

17. M. UCHIDA, H.-M. KIM, F. MIYAJI, T. KOKUBO and T. NAKAMURA, *Biomaterials* **23** (2002) 313

18. T. KOKUBO and H. TAKADAMA, *Biomaterials* **27** (2006) 2907

19. K. TSURU, C. OHTSUKI, A. OSAKA, T. IWAMOTO and J. D. MACKENZIE, *J. Mater. Sci-Mater. M.* **8** (1997) 157

20. J. D. FERRY, In *Viscoelastic Properties of Polymers*, 3rd ed (New York: Wiley, 1980)

21. S. B. ADALJA and J. U. OTAIGBE, *Polym. Composit.* **23** (2002) 171

22. H. LU, B. WANG, J. MA, G. HUANG and H. VISWANATHAN, In *Mechanics of The Time-Dependent Materials*, vol. 7 (2003) p. 189

23. M. R. VANLANDINGHAM, J. S. VILLARUBIA, W. F. GUTHRIE and G. F. MEYERS, *Macromol. Symp.* **167** (2001) 15

24. M. KRUK and M. JARONIEC, *Chem. Mater.* **13** (2001) 3169

25. H.-P. LIN, S.-T. WONG, C.-Y. MOU and C.-Y. Tang, *J. Phys. Chem.B* **104** (2000) 8967

26. L. ESQUIVIAS and N. DE LA ROSA-FOX, *J. Sol-Gel Sci. Technol.* **26** (2002) 651

27. N. DE LA ROSA-FOX, L. ESQUIVIAS and M. PIÑERO, "Organic-Inorganic Hybrid Materials from Sonogels" In *Handbook of Organic-Inorganic Hybrid Materials and Nanocomposites*, edited by S. H. NALWA, vol. 1 (American Scientific Publishers, Ca., 2003) p. 241

28. V. MORALES-FLÓREZ, Modelos Estructurales y Propiedades Mecánicas de Aerogeles Híbridos. Ph. D Thesis, University of Seville, Spain, 2007

29. X. LIU, CH. DING and P. K. CHU, *Biomaterials* **25** (2004) 1755

30. X. LIU, CH. DING and Z. WANG, *Biomaterials* **22** (2001) 2007

31. P. SARAVANAPAVAN and L. L. HENCH, *J. Non-Cryst. Solids* **318** (2003) 1

32. T. YABUTA, K. TSURU, S. HAYAKAWA and A. OSAKA, *J. Sol-Gel Sci. Techn.* **31** (2004) 273

33. C. D. VOLPE, S. DIRÉ and E. PAGANI, *J. Non-Cryst. Solids* **209** (1997) 51

34. M. FUKUSHIMA, E. YASUDA, H. KITA, M. SHIMIZU, Y. HOSHIKAWA and Y. TANABE, In "Proceedings of the 29th International Conference on Advanced Ceramics and Composites-Advances in Bioceramics and Biocomposites", edited by M. MISUNO (2005) p. 103

35. R. O. R. COSTA, M. M. PEREIRA, F. S. LAMEIRAS and W. L. VASCONCELOS, *J. Mater. Sci.-Mater. M* **16** (2005) 927

36. M. MANZANO, A. J. SALINAS and M. VALLET-REGÍ, *Prog. Solid State Ch.* **34** (2006) 267

37. Y.R. DUAN, Z. R. ZHANG, C. Y. WANG, J. Y. CHEN and X. D. ZHANG, *J. Mater. Sci.-Mater. M* **16** (2005) 795

38. A. RÁMILA and M. VALLET-REGÍ, *Biomaterials* **22** (2001) 2301

39. M. KAMITAKAHARA, M. KAWASHITA, N. MIYATA, T. KOKUBO and T. NAKAMURA, *J. Mater. Sci.-Mater. M* **13** (2002) 1015

40. M. P. MAHABOLE, R. C. AIYER, C. V. RAMAKRISHNA, B. SREEDHAR and R. S. KHAIRNAR, *Bull. Mater. Sci.* **28** (2005) 535

41. S. PADILLA, J. ROMÁN, A. CARENAS and M. VALLET-REGÍ, *Biomaterials* **26** (2005) 475

42. L. L. HENCH, J. WILSON In *An introduction to bioceramics*, edited by L. L. HENCH, J. WILSON (World Scientific, Singapore, 1993), p. 12

43. T. KOKUBO, H.-M. KIM and M. KAWASHITA, *Biomaterials.* **24** (2003) 2161

44. N. DE LA ROSA-FOX, V. MORALES-FLÓREZ, J. A. TOLEDO-FERNÁNDEZ, M. PIÑERO, R. MENDOZA-SERNA and L. ESQUIVIAS, *J. Eur. Cer. Soc.* **27** (2007) 3311